The influence of water on the strength of Neapolitan Yellow Tuff, the most widely-used building stone in Naples (Italy)

Michael J. Heap*[1], Jamie I. Farquharson[1], Alexandra R. L. Kushnir[1], Yan Lavallée[2], Patrick Baud[1], H. Albert Gilg[3], and Thierry Reuschlé[1]

[1]*Géophysique Expérimentale, Institut de Physique de Globe de Strasbourg (UMR 7516 CNRS, Université de Strasbourg/EOST), 5 rue René Descartes, 67084 Strasbourg cedex, France.*

[2]*Earth, Ocean and Ecological Sciences, University of Liverpool, Liverpool L693GP, United Kingdom.*

[3]*Lehrstuhl für Ingenieurgeologie, Technische Universität München, Munich, Germany.*

Corresponding author: Michael Heap (heap@unistra.fr)

Abstract

Neapolitan Yellow Tuff (NYT) has been used in construction in Naples (Italy) since the Greeks founded the city—then called Neapolis—in the 6th century BCE. We investigate here whether this popular building stone is weaker when saturated with water, an issue important for assessments of weathering damage and monument preservation. To this end, we performed 28 uniaxial compressive strength measurements on dry and water-saturated samples cored from a block of the lithified Upper Member of the NYT. Our experiments show that the strength of the zeolite-rich NYT is systematically reduced when saturated with water (the ratio of wet to dry

strength is 0.63). Complementary experiments show that two other common Neapolitan building stones—Piperno Tuff and the grey Campanian Ignimbrite (both facies of the Campanian Ignimbrite deposit devoid of zeolites)—do not weaken when wet. From these data, and previously published data for tuffs around the globe, we conclude that the water-weakening in NYT is a consequence of the presence of abundant zeolites (the block tested herein contains 46 wt.% of zeolites). These data may help explain weathering damage in NYT building stones (due to rainfall, rising damp, and proximity to the sea or water table) and the observed link between rainfall and landslides, rock falls, and sinkhole formation in Naples, and the weathering of other buildings built from zeolite-rich tuffs worldwide.

Keywords: zeolites; uniaxial compressive strength; porosity; mercury porosimetry

1 Introduction

For millennia, tuffs have been used worldwide as a building stone (Heiken, 2006). Cities built on and constructed using tuff span six of the seven continents (all except Antarctica). Tuff has been used as a building material in Naples (Italy; Figure 1) since the city's birth as Neapolis in the 6th century BCE (e.g., Calcaterra et al., 2000; de'Gennaro et al., 2000a; Evangelista et al., 2000a; Colella et al., 2001, Calcaterra et al., 2005; Morra et al., 2010; Aversa et al., 2013; Colella et al., 2017). The most commonly used tuff in Naples is the Neapolitan Yellow Tuff (NYT), the product of a large phreatoplinian eruption from the adjacent Campi Flegrei volcanic district (e.g., Orsi et al., 1992; Scarpati et al., 1993; Wohletz et al., 1995; Orsi et al., 1996; Civetta et al., 1997) about 15,000 years ago (Deino et al., 2004). However, laboratory experiments on tuff show that they are sometimes weaker when saturated

with water (e.g., Schultz and Li, 1995; Yassaghi et al., 2005; Jackson et al., 2005; Montanaro et al., 2016). The metric "water-weakening", the ratio of the wet to dry strength of a material, is often used to describe this affect (Zhu et al., 2011), where low values (close to zero) indicate a strong water-weakening effect and values at or close to unity indicate that there is little or no water-weakening. A water-weakening assessment of the NYT is particularly important due to the prevalence of water related weathering typologies seen on buildings in Naples (e.g., de'Gennaro et al., 1993, 2000a; Di Benedetto et al., 2015).

The stratigraphy of the NYT is divided into two members: a Lower Member (comprising fall deposits and pyroclastic flow deposits) and an Upper Member (comprising pyroclastic flow deposits) (Scarpati et al., 1993; Cole and Scarpati, 1993). The Upper Member is composed of the deposits of a non-turbulent pyroclastic density flow and five low- and high-concentration turbulent pyroclastic density flows (Cole and Scarpati, 1993). The Upper Member is variably lithified and is preserved as either unlithified grey "pozzolana" material or a lithified yellow rock (e.g., Scarpati et al., 1993; Cole and Scarpati, 1993; de'Gennaro et al., 2000b). The lithified Upper Member has been divided into four texturally distinct units, classified by the size and quantity of lithic and porous juvenile fragments (Colella et al., 2017). The lithified Upper Member of the NYT has not only been used in the construction of monuments such as Castel dell'Ovo, Castel Nuovo, the churches of Santa Chiara and San Domenico Maggiore, and the Academy of Fine Arts, but also in many of the walls and houses within the ancient city centre of Naples (Figure 2).

The lithified Upper Member of the NYT is a particularly well-studied material, for a number of reasons. First, due to its prevalent use in construction in the Neapolitan area (de'Gennaro et al., 1993; Aversa and Evangelista, 1998; de'Gennaro

et al., 2000a; Evangelista et al., 2000a; Augenti and Parisi, 2010; Nijland et al., 2010; Calderoni et al., 2010; Heap et al., 2012; Di Benedetto et al., 2015; La Russa et al., 2017; Colella et al., 2017). Second, due to alarming frequency of landslide and rock fall hazards (Calcaterra et al., 2002; Di Martire et al., 2002; Calcaterra et al., 2007; Nocilla et al., 2009) and underground cavity collapse and anthropogenic sinkhole formation (Evangelista et al., 2000b; Hall et al., 2005; Guarino and Nisio, 2012; Guarino et al., 2018) associated with the NYT. Third, the NYT contains abundant zeolites, aluminosilicate minerals of commercial, industrial, and environmental importance (de'Gennaro et al., 1990, 2000a; Coppola et al., 2002; Colella, 2005). Finally, since NYT is one of the principal lithologies forming the increasingly restless Campi Flegrei caldera (Orsi et al., 1996; Di Vito et al., 1999; Chiodini et al., 2001; Heap et al., 2014; Chiodini et al., 2015; Mayer et al., 2016; Montanaro et al., 2016; Kilburn et al., 2017; Chiodini et al., 2017; Cardellini et al., 2017), a detailed understanding of the physical and mechanical properties of the NYT form an important component of volcanic risk assessment and mitigation.

These studies, amongst others, have shown that the lithified Upper Member of the NYT is a heterogeneous trachytic pyroclastic deposit that is characterised by both pyrogenic and authigenic phases (de'Gennaro et al., 1990). It contains variably quantities of porous juvenile lapilli (i.e., pumice) fragments (between ~8 and ~40%) and lithic fragments (between ~7 and ~16%) (Colella et al., 2017). The NYT typically contains a large proportion of plagioclase phenocrysts (between ~14 and ~36 wt.%; Colella et al., 2017), amorphous phases (~10 wt.%; Di Benedetto et al., 2015; Colella et al., 2017), and zeolites, namely K-rich phillipsite, chabazite, and analcime (Gatta et al., 2010; Heap et al., 2012; Di Benedetto et al., 2015; Colella et al., 2017). The mean content of zeolites within the NYT can exceed 50 wt.% (de'Gennaro et al., 1990,

2000a; Di Benedetto et al., 2015; Colella et al., 2017). Also found within the NYT are subordinate smectite (between 0 and 6 wt.%; Di Benedetto et al., 2015; Colella et al., 2017) and phenocrysts of sanidine, clinopyroxene, biotite, and minor quantities of Ti-magnetite and apatite (Heap et al., 2012; Di Benedetto et al., 2015).

Due to the heterogeneity of the lithified Upper Member of the NYT (e.g., Scarpati et al., 1993; Cole and Scarpati, 1993; Colella et al., 2017), its physical properties are equally heterogeneous. For example, its porosity and permeability can range from 0.35 and 0.65 (Colella et al., 2017) and 10^{-17} and 10^{-13} m^2 (Peluso and Arienzo, 2007; Heap et al., 2014; Montanaro et al., 2016), respectively. Reported values of uniaxial compressive strength (UCS) of NYT typically vary between ~1 and ~10 MPa, although it can be as strong as ~40 MPa (Evangelista and Aversa, 1994; Hall et al., 2005; Augenti and Parisi, 2009; Heap et al., 2012; Montanaro et al., 2016; Colella et al., 2017). Further, and due to its high porosity, triaxial deformation experiments have shown that NYT is compactant (i.e. ductile) even at very low effective pressures (< 5 MPa) and under ambient laboratory temperatures (Aversa and Evangelista, 1998; Heap et al., 2014).

The physical and mechanical properties of tuffs are well known to be influenced by exposure to the elements, as recognised by Vitruvius as far back as pre-Christian Rome (Italy), where he wrote: "*There are also many other kinds, such as red and black tuff in Campania, [and] in Umbria, Piceno and in Venetia white, which, indeed, can be cut like wood by means of a serrated or toothed saw. So long as these soft stones are sheltered under plaster they will hold up and do their work but if they are laid bare or exposed in the open air, ice and frost accumulate within them and they crumble apart and dissolve. Also along the sea coast salt eats at them and they dissolve apart; neither do they endure sea tides and spray.*" (from De

126 Architectura 2.7.1-2 as quoted in Jackson et al., 2006). Indeed, and more recently,
127 NYT has been shown to degrade during salt crystallization tests (La Russa et al.,
128 2017) and the UCS and indirect tensile strength of zeolite-rich NYT was found to
129 decrease following exposure to the high-temperatures of fire (Heap et al., 2012).
130 However, since the early work of Evangelista (1980), an unpublished report
131 containing experiments that show that the peak strength of NYT is reduced when
132 water-saturated, the water-weakening behaviour of the lithified Upper Member of the
133 NYT has received little attention in the literature. To the authors' knowledge, only
134 Montanaro et al. (2016) provide a handful of UCS experiments (three dry and three
135 water-saturated) that show that NYT is weaker when saturated with water (dry UCS =
136 6.1-7.3 MPa; wet UCS = 1.2-2.3 MPa). The lack of a comprehensive study is
137 surprising on two counts. First, deformation experiments on tuffs have highlighted
138 that they are weaker when saturated with water (e.g., Schultz and Li, 1995; Yassaghi
139 et al., 2005; Jackson et al., 2005; Montanaro et al., 2016). Second, a survey of
140 weathering typologies in buildings in Naples constructed with NYT found that the
141 most prevalent weathering type was the result of moisture (due to rising damp) and
142 rainfall (de'Gennaro et al., 2000a). This type of weathering results in alveolisation
143 (detachment of lithic and porous juvenile fragments), scaling, exfoliation, and
144 disaggregation, as shown in Figure 3 (see also de'Gennaro et al., 1993, 2000a; Di
145 Benedetto et al., 2015). We thus report, herein, on the results of an experimental study
146 that quantifies the water-weakening behaviour of a facies of the NYT often used in
147 construction in the Neapolitan area.
148

149 **2 Experimental material and methods**

We performed uniaxial compressive strength (UCS) measurements on cylindrical samples of NYT cored in the same orientation from a single block. The block of NYT (from the lithified yellow Upper Member) was sourced from an open quarry at Monte San Severino, at the boundary of the inferred Campi Flegrei caldera (the same block used in Heap et al., 2012, 2014; see Figure 1 for sample location). Importantly, this quarry has supplied dimension stones (natural stone or rock that has been selected and finished to a specific size or shape) for building projects within the Neapolitan area. Due to the presence of centimetric juvenile lapillis, the NYT tested herein is similar to the facies "MC" described by Colella et al. (2017).

A total of 28 samples were cored to a diameter of either 25 or 20 mm and cut and precision-ground to a nominal length of 60 or 40 mm, respectively (a photograph of a 20 mm-diameter sample is provided as Figure 4a). Samples were cored so as to avoid centimetric juvenile lapillis and lithic fragments. To avoid the washout of juvenile lapilli and the fine fraction, the sample block was first soaked in water and then cored dry (i.e., samples were cored without running water). The prepared cylindrical samples were then washed with water to remove any water-soluble grinding fluid and vacuum-dried in an oven for at least 48 hours at 40 °C. The connected porosity of each sample was then determined using the skeletal (connected) volume of the sample given by a helium pycnometer (Micromeritics AccuPyc II 1340) and the bulk volume of the sample calculated using the sample dimensions. Finally, the samples were deformed uniaxially at a strain rate of 1.0×10^{-5} s^{-1} until macroscopic failure. Thirteen of the samples were deformed "dry" (dried in a vacuum-oven for at least 48 hours prior to deformation) and 15 were deformed "wet" (vacuum-saturated in deionised water and deformed in a water bath). The water

saturation procedure for the samples deformed in the "wet" condition consisted of two steps:

(1) the vacuum-dried samples were placed inside a belljar which was then vacuumed for at least 12 h and, finally,

(2) degassed (using a Venturi siphon with municipal water as the motive fluid) deionised water was introduced into the belljar whilst under vacuum.

A mercury injection test was performed on a small vacuum-dried offcut (~3.5 g) of NYT using the Micromeritics Autopore IV 9500 at the University of Aberdeen (Scotland). The evacuation pressure and evacuation time were 50 μm Hg and 5 min, respectively, and the mercury filling pressure and equilibration time were 3.59 MPa and 10 s, respectively. The pressure range was 0.69 to 413.69 MPa. Mercury injection data permit the estimation of connected porosity and pore throat size distribution. The mercury injection data were corrected for the "low pressure correction" recommended by the American Section of the International Association for Testing Materials (ASTM D4404-10).

The mineral content of the studied NYT was quantified using X-ray powder diffraction (XRPD). A powder, prepared from the deformed NYT cores and containing 10 wt.% ZnO as internal standard, was ground for 8 min with 10 ml of isopropyl alcohol in a McCrone Micronising Mill using agate cylinder elements. The XRPD analyses were performed on powder mounts using a PW 1800 X-ray diffractometer (CuKα, graphite monochromator, 10 mm automatic divergence slit, step-scan 0.02° with 2θ increments per second, counting time one second per increment, 30 mA, 40 kV). The phases in the whole rock powders were quantified using the Rietveld program BGMN (Bergmann et al., 1998). To identify the clay minerals, we also separated <2 μm fractions by gravitational settling and prepared

oriented mounts that were X-rayed in an air-dried and ethylene-glycolated state. Since some of the constituents of the NYT are delicate (juvenile lapilli), and/or may be affected by vacuum-drying (zeolites and clays), we chose to prepare our powdered sample for XRPD analysis using the deformed core samples so that the mineral content determined is representative of the deformed samples, rather than the block prior to sample preparation. Although our samples were prepared with the utmost care, we cannot definitively rule out that their mineral content was slightly modified by the sample preparation procedure.

3 Results

3.1 Mineral content and microstructure

The microstructure of the NYT used in this study contains phenocrysts (of K-feldspar, clinopyroxene, and biotite) and juvenile lapilli within a fine-grained matrix (Figure 4b). Table 1 gives the XRPD analysis, which shows that the main minerals within the NYT are amorphous phases (36 wt.%, Table 1) and two zeolites: chabazite (30 wt.%, Table 1) and phillipsite (16 wt.%, Table 1). The block of NYT also contains 10 wt.% K-feldspar, 3 wt.% clinopyroxene, 3 wt.% smectite, and 2 wt.% biotite (Table 1). The total proportion of zeolites (chabazite and phillipsite) is therefore 46 wt.%. We note that the amorphous phase (36 wt.%, Table 1) measured is likely to contain little residual glass (Colella et al., 2017) and could include an aluminosilicate gel-like component (de'Gennaro and Colella, 1989; Colella et al., 2017).

3.2 Experimental data

223 The NYT studied has an average dry bulk density of 1,240 kg.m^{-3} and an
224 average connected porosity of 0.458 (standard deviation: 0.0079) (Table 2). A
225 connected porosity of 0.446 was determined from the mercury injection data. The
226 pore throat size distribution for NYT is shown in Figure 5a. These data show that pore
227 throats of diameter ≥ 10 μm constitute ~10% of the pores by volume (Figure 5a). The
228 majority of pores (~65%) have a diameter between 0.3 and 3 μm (Figure 5a). The
229 average pore throat diameter was determined to be 0.21 μm.

230 Representative uniaxial stress-strain curves for dry and wet NYT samples are
231 shown in Figure 5b, and the UCS is plotted as a function of connected porosity in
232 Figure 5c (data given in Table 2). The average wet and dry strength was found to be
233 3.50 and 5.58 MPa, respectively. The ratio of wet to dry strength—a metric
234 commonly used to assess water-weakening in rocks (Zhu et al., 2011)—is 0.63.

235

236 **4 Discussion**

237 We have performed UCS tests on cylindrical cores of dry and water-saturated
238 NYT either 20 or 25 mm in diameter. Although these diameters are standard in
239 volcanological studies, the strength of engineering materials is typically determined
240 on samples that are 50 mm in diameter. Due to the influence of sample geometry on
241 the UCS (Hawkes and Mellor, 1970; Hoek and Brown, 1980), we provide here UCS
242 values for 50 mm-diameter core samples using the following empirical relation (Hoek
243 and Brown, 1980):

244

$$UCS = UCS_{50}\left(\frac{50}{d}\right)^{0.18}, \quad (1)$$

245

where UCS is the uniaxial compressive strength measured for a cylindrical sample of diameter d (in mm) and UCS_{50} is the uniaxial compressive strength of a 50 mm-diameter core sample. The UCS_{50} values for our experiments are given in Tables 2 and 5. However, although this allows us to better compare our UCS values with those from the engineering literature, we highlight that the goal of this contribution was to understand whether NYT is weaker when water-saturated. In this case, the metric of interest—the ratio of wet to dry UCS—is independent of sample diameter.

Our data show that the UCS of water-saturated NYT is weaker than dry NYT (Figure 5c). These data are in accordance with tuffs sourced from Italy and elsewhere. For example, studies have shown that the tuffs from the Cappadocia (Erdoğan, 1986; Erguvanlı et al., 1989; Topal and Doyuran, 1997; Tuncay, 2009; Erguler and Ulusay, 2009) and Afyonkarahisar (Çelik et al., 2014; Çelik and Ergul, 2015) regions of Turkey, tuffs from different locations in Hungary (Vásárhelyi, 2002), and tuffs from Rome (Jackson et al., 2005) and the Neapolitan area (Montanaro et al., 2016; Marmoni et al., 2017a) are weaker when wet. To test the hypothesis that the presence of zeolites and/or clays is responsible for the observed water-weakening in tuffs, we have collated the available published data on the wet versus dry compressive (Table 3) and tensile (Table 4) strength of tuffs from around the world (Figure 6). All the data are presented in Figure 6a, and Figure 6b shows only UCS data for which the composition is known. The data in Figure 6b have been divided into three groups: (1) tuffs that contain zeolites, (2) tuffs that contain clays but no zeolites, and (3) tuffs that contain neither zeolites nor clays.

To complement these data, we performed ancillary experiments on two tuffs that contain no zeolites or clays – the grey Campanian Ignimbrite (welded grey ignimbrite, WGI) and the Piperno Tuff (PT). Both rocks are facies of the Campanian

Ignimbrite deposit (e.g., Barberi et al., 1978; Rosi et al., 1996; Fedele et al., 2016) and have been used in construction within the Neapolitan area (e.g., Calcaterra et al., 2000; de'Gennaro et al., 2000a; Calcaterra et al., 2005; Morra et al., 2010). The use of PT is particularly widespread in the ancient city centre of Naples, the church of Gesù Nuovo providing a spectacular example (Figure 7). Piperno Tuff was also used to construct the corner towers of Castel Nuovo (Figure 2b). Cylindrical samples (20 mm in diameter and nominally 40 mm in length) were prepared from both the WGI block described in Heap et al. (2012, 2014) and the PT block described in Heap et al. (2012), as described in the methods section above. The WGI samples tested contain hypidiomorphic phenocrysts of alkali feldspar with minor clinopyroxene within a matrix composed of microlites of alkali feldspar, Ti-magnetite, and apatite, as well as well-sorted glass shards with occasional accretionary ash clots and porous lapilli fragments (Heap et al., 2012). Piperno Tuff is characterised by a eutaxitic texture with black flattened scoriae and phenocrysts of alkali feldspar and clinopyroxene set within a light grey matrix of well-sorted glass shards and microlites of alkali feldspar and Ti-magnetite (Heap et al., 2012). Importantly, no zeolites or clays are present within these blocks (see XRD data presented in Heap et al., 2012). The connected porosities of the WGI and PT samples were first determined; the samples were then deformed in either the dry or wet condition (as described in the methods section above). The results of these experiments are summarised in Table 5. The ratio of wet to dry strength in WGI and PT is 0.939 and 1.038, respectively (Figure 6b; Table 3). In other words, based on these data, WGI and PT are not weaker in the presence of water.

Figure 6b suggests that the presence of zeolites and clays promote water-weakening in tuffs, although firm conclusions cannot be drawn due to the paucity of data for zeolite-free tuff. The four samples of zeolite-free tuff (Karaj (crystalline),

296 Cappadoccian (Kızılkaya), the WGI, and the PT) show consistently high ratios of
297 UCS_{wet}/UCS_{dry} – between ~0.6 and ~1.0 (Figure 6b; Table 3). By contrast, zeolite-
298 and clay-bearing tuffs have average UCS_{wet}/UCS_{dry} ratios of 0.54 and 0.37,
299 respectively (Figure 6b; Table 3). We therefore conclude that the water-weakening in
300 NYT is the result of the presence of abundant zeolites (46 wt.% in total; Table 1),
301 although the influence of subordinate clay (3 wt.%; Table 1), thought to promote
302 water-weakening in sandstones (Dyke and Dobereiner, 1991; Schmitt et al., 1994;
303 Demarco et al., 2007; Shakoor and Barefield, 2009), cannot be discounted. We
304 attribute the observed weakening in the presence of water to the hydric expansion of
305 zeolites and clays (e.g., Nijland et al., 2010; Wedekind et al., 2013; López-Doncel et
306 al., 2013). However, based on the available data, we cannot definitively rule out the
307 influence of porosity type (pores versus microcracks), pore shape, average pore size,
308 and pore size distribution, amongst others, on the water-weakening behaviour of tuffs.
309 Indeed, Wedekind et al. (2013) found a correlation between microporosity, average
310 pore radius, and moisture expansion for a variety of tuffs from Mexico, Germany, and
311 Hungary.

312 We also highlight that, in our study, we compare the strength of dry and fully
313 saturated samples. In reality, it is unlikely that building stones will be fully-saturated
314 with water. However, experimental studies have shown that even low levels of water
315 saturation can result in measurable water-weakening in tuffs (Kleb and Vásárhelyi,
316 2003; Çelik and Ergül, 2015). For example, Çelik and Ergül (2015) found that
317 immersion in water for 1 h was sufficient to reduce the strength of tuff by ~32%.
318 Water-weakening at low levels of water saturation has also been observed in clay-rich
319 sandstones (Dyke and Dobereiner, 1991; Schmitt et al., 1994; Demarco et al., 2007;
320 Shakoor and Barefield, 2009). Therefore, we consider our conclusions, drawn from

experiments on dry and fully saturated samples, are relevant for monuments and buildings constructed using NYT. We further note that we have only tested one facies of the heterogeneous lithified Upper Member of the NYT (Colella et al., 2017). However, yellow-coloured tuffs associated with more recent (post-NYT) eruptions at Campi Flegrei (Gauro and La Pietra Tuffs) also show water-weakening (Montanaro et al., 2016; Table 3). Importantly, these tuffs are texturally different to the facies studied herein. Indeed, one of the La Pietra Tuffs contained very few lapilli-sized lithic and porous juvenile fragments (similar to the "NP" end-member facies of the NYT reported in Colella et al., 2017). Based on these data, we expect the NYT facies that are texturally different to that studied herein will also be weaker when wet (as long as they contain zeolites), although more experiments should now be performed to test this hypothesis.

5 Conclusions

We have shown that a block of the lithified Upper Member of the NYT, often used in construction within the Neapolitan region of Italy, is weaker when water-saturated (Figure 5c). Compiled data on the wet and dry strength of tuffs from across the globe suggest that the cause of the water-weakening is the due to the presence of zeolites (Figure 6b). Water-weakening in the zeolite-rich NYT may help explain the widespread weathering observed in Naples due to moisture (as a result of rising damp) and rainfall (Figure 3; de'Gennaro et al., 1993, 2000a; Di Benedetto et al., 2015) and the apparent link between rainfall and landslide and rock fall hazards (Calcaterra et al., 2002; Di Martire et al., 2002; Calcaterra et al., 2007; Nocilla et al., 2009) and sinkhole formation (Guarino and Nisio, 2012). We additionally conclude that the buildings constructed using zeolite-free tuffs, such as the church of Gesù

Nuovo (Figure 7), will be less prone to weathering associated with moisture and rainfall. This latter hypothesis is supported by the observation that, while the WGI is only subject to physical weathering, the zeolitised facies of the Campanian Ignimbrite is more affected by chemical action (de'Gennaro et al., 1995). We anticipate that the implications of this study will be important not only for building and monument preservation in Naples, but also in other cities worldwide constructed using tuff.

Acknowledgements

This work was funded in part by the "Partenariats Hubert Curien (PHC) GALILEE 2016-2017" grant (project number 37180VC) "Landslide-triggered tsunami hazard in the Mediterranean: improving risk mitigation strategies by understanding natural processes", implemented by, in France, the Ministry of Europe and Foreign Affairs (MEAE) and the Ministry of Higher Education, Research and Innovation (MESRI) and, in Italy, the Franco-Italian University (UFI) and the Ministry of Education, Universities and Research (MIUR). We wish to thank Bertrand Renaudié for laboratory assistance. We thank Giovanni Orsi for providing the experimental materials, and Balázs Vásárhelyi and Cristian Montanaro for helpful discussions. We also acknowledge the work of the archivists of the Internet Archive digital library (https://archive.org). We are grateful for the constructive comments of two anonymous reviewers, the editor (Laura Pioli), and the executive editor (Andrew Harris). We also thank Marie Jackson and John Oleson for discussions on the texts of Vitruvius.

References

ASTM D4404-10, Standard Test Method for Determination of Pore Volume and Pore Volume Distribution of Soil and Rock by Mercury Intrusion Porosimetry, ASTM International, West Conshohocken, PA, 2010, www.astm.org.

Augenti, N., & Parisi, F. (2009). Mechanical characterization of tuff masonry. Proc. Of Protection of Historical Buildings, PROHITECH, 9, 1579-1584.

Augenti, N., & Parisi, F. (2010). Constitutive models for tuff masonry under uniaxial compression. Journal of Materials in Civil Engineering, 22(11), 1102-1111.

Aversa, S., & Evangelista, A. (1998). The mechanical behaviour of a pyroclastic rock: yield strength and "destructuration" effects. Rock Mechanics and Rock Engineering, 31(1), 25-42.

Aversa, S., Evangelista, A., & Scotto Di Santolo, A. (2013). Influence of the subsoil on the urban development of Napoli. In Proc. Of the 2nd Int. Symp. On Geotechnical Engineering for the Preservation of Monuments and Historic Sites, 15-43.

Ayday, C., & Göktan, R. M. (1990). A preliminary engineering geology study directed to the conservation of Midas monument. In Proc. International Earth Sciences Colloquium on the Aegean Region (IESCA), DE University, Izmir (pp. 102-108).

Barberi, F., Innocenti, F., Lirer, L., Munno, R., Pescatore, T., & Santacroce, R. (1978). The Campanian Ignimbrite: a major prehistoric eruption in the Neapolitan area (Italy). Bulletin Volcanologique, 41(1), 10-31.

Behre Jr., C. D. (1929). Volcanic Tuffs and Sandstones used as building stones in the upper Salmon River Valley, Idaho. Contributions to Economic Geology, Part 1.

Calcaterra, D., Cappelletti, P., Langella, A., Morra, V., Colella, A., & de Gennaro, R. (2000). The building stones of the ancient centre of Naples (Italy): Piperno from Campi Flegrei. A contribution to the knowledge of a long-time-used stone. Journal of Cultural Heritage, 1(4), 415-427.

Calcaterra, D., De Riso, R., Nave, A., & Sgambati, D. (2002). The role of historical information in landslide hazard assessment of urban areas: the case of Naples (Italy). In Proc. 1st European Conference on Landslides, Prague (pp. 129-135).

Calcaterra, D., Langella, A., De Gennaro, R., de'Gennaro, M., & Cappelletti, P. (2005). Piperno from Campi Flegrei: a relevant stone in the historical and monumental heritage of Naples (Italy). Environmental geology, 47(3), 341-352.

Calcaterra, D., Coppin, D., De Vita, S., Di Vito, M. A., Orsi, G., Palma, B., & Parise, M. (2007). Slope processes in weathered volcaniclastic deposits within the city of Naples: The Camaldoli Hill case. Geomorphology, 87(3), 132-157.

Calderoni, B., Cecere, G., Cordasco, E. A., Guerriero, L., Lenza, P., & Manfredi, G. (2010). Metrological definition and evaluation of some mechanical properties of post-medieval Neapolitan yellow tuff masonry. Journal of Cultural Heritage, 11(2), 163-171.

Cardellini, C., Chiodini, G., Frondini, F., Avino, R., Bagnato, E., Caliro, S., Lelli, M., & Rosiello, A. (2017). Monitoring diffuse volcanic degassing during volcanic unrests: the case of Campi Flegrei (Italy). Scientific Reports, 7.

Çelik, M. Y., Akbulut, H., & Ergül, A. (2014). Water absorption process effect on strength of Ayazini tuff, such as the uniaxial compressive strength (UCS), flexural strength and freeze and thaw effect. Environmental Earth Sciences, 71(9), 4247-4259.

Çelik, M. Y., & Ergül, A. (2015). The influence of the water saturation on the strength of volcanic tuffs used as building stones. Environmental Earth Sciences, 74(4), 3223-3239.

Chiodini, G., Frondini, F., Cardellini, C., Granieri, D., Marini, L., & Ventura, G. (2001). CO2 degassing and energy release at Solfatara volcano, Campi Flegrei, Italy. Journal of Geophysical Research: Solid Earth, 106(B8), 16213-16221.

Chiodini, G., Vandemeulebrouck, J., Caliro, S., D'Auria, L., De Martino, P., Mangiacapra, A., & Petrillo, Z. (2015). Evidence of thermal-driven processes triggering the 2005–2014 unrest at Campi Flegrei caldera. Earth and Planetary Science Letters, 414, 58-67.

Chiodini, G., Selva, J., Del Pezzo, E., Marsan, D., De Siena, L., D'Auria, L., Bianco, F., Caliro, S., De Martino, P., Ricciolino, P., & Petrillo, Z. (2017). Clues on the origin of post-2000 earthquakes at Campi Flegrei caldera (Italy). Scientific reports, 7.

Civetta, L., Orsi, G., Pappalardo, L., Fisher, R. V., Heiken, G., & Ort, M. (1997). Geochemical zoning, mingling, eruptive dynamics and depositional processes—the Campanian Ignimbrite, Campi Flegrei caldera, Italy. Journal of Volcanology and Geothermal Research, 75(3), 183-219.

Colella, C., de'Gennaro, M., & Aiello, R. (2001). Use of zeolitic tuff in the building industry. Reviews in Mineralogy and Geochemistry, 45(1), 551-587.

Colella, C. (2005). Natural zeolites. Stud Surf Sci Catal, 157, 13-40.

Colella, A., Di Benedetto, C., Calcaterra, D., Cappelletti, P., D'Amore, M., Di Martire, D., Graziano, S. F., Papa, L., de Gennaro, M., & Langella, A. (2017). The Neapolitan Yellow Tuff: An outstanding example of heterogeneity. Construction and Building Materials, 136, 361-373.

Coppola, E., Battaglia, G., Bucci, M., Ceglie, D., Colella, A., Langella, A., ... & Colella, C. (2002). Neapolitan yellow tuff for the recovery of soils polluted by potential toxic elements in illegal dumps of Campania Region. Studies in Surface Science and Catalysis, 142, 1759-1766.

Deino, A. L., Orsi, G., de Vita, S., & Piochi, M. (2004). The age of the Neapolitan Yellow Tuff caldera-forming eruption (Campi Flegrei caldera–Italy) assessed by 40 Ar/39 Ar dating method. Journal of Volcanology and Geothermal Research, 133(1), 157-170.

de'Gennaro, M., & Colella, C. (1989). Use of thermal analysis for the evaluation of zeolite content in mixtures of hydrated phases. Thermochimica Acta, 154(2), 345-353.

de'Gennaro, M., Fuscaldo, M. D., & Colella, C. (1993). Weathering mechanisms of monumental tuff-stone masonries in downtown Naples. Science and Technology for Cultural Heritage, 2, 53-62.

de'Gennaro, M., Colella, C., Langella, A., Cappelletti, P. (1995). Decay of Campanian Ignimbrite stoneworks in some monuments of the Caserta area. Science and Technology for Cultural Heritage, 4, 75-86.

de'Gennaro, M., Calcaterra, D., Cappelletti, P., Langella, A., & Morra, V. (2000a). Building stone and related weathering in the architecture of the ancient city of Naples. Journal of Cultural Heritage, 1(4), 399-414.

de'Gennaro, M., Cappelletti, P., Langella, A., Perrotta, A., & Scarpati, C. (2000b). Genesis of zeolites in the Neapolitan Yellow Tuff: geological, volcanological and mineralogical evidence. Contributions to Mineralogy and Petrology, 139(1), 17-35.

Demarco, M. M., Jahns, E., Rüdrich, J., Oyhantcabal, P., & Siegesmund, S. (2007). The impact of partial water saturation on rock strength: an experimental study on sandstone [Der Einfluss einer partiellen Wassersättigung auf die mechanischen Gesteinseigenschaften: eine Fallstudie an Sandsteinen]. Zeitschrift der Deutschen Gesellschaft für Geowissenschaften, 158(4), 869-882.

Di Benedetto, C., Cappelletti, P., Favaro, M., Graziano, S. F., Langella, A., Calcaterra, D., & Colella, A. (2015). Porosity as key factor in the durability of two historical building stones: Neapolitan Yellow Tuff and Vicenza Stone. Engineering Geology, 193, 310-319.

Di Martire, D., De Rosa, M., Pesce, V., Santangelo, M. A., & Calcaterra, D. (2012). Landslide hazard and land management in high-density urban areas of Campania region, Italy. Natural Hazards and Earth System Sciences, 12(4), 905.

Di Vito, M. A., Isaia, R., Orsi, G., Southon, J., De Vita, S., d'Antonio, M., Pappalardo, L., & Piochi, M. (1999). Volcanism and deformation since 12,000 years at the Campi Flegrei caldera (Italy). Journal of Volcanology and Geothermal Research, 91(2), 221-246.

Dyke, C. G., & Dobereiner, L. (1991). Evaluating the strength and deformability of sandstones. In Quarterly Journal of Engineering Geology and Hydrogeology (Vol. 24, No. 1, pp. 123-134). Geological Society of London.

Erdoğan M. (1986). Nevşehir-Ürgup yöresi tüflerinin malzeme jeolojisi açısından araştırılması. Unpublished doctoral dissertation, Istanbul Technical University (ITU), Faculty of Mining, Istanbul.

Erguler, Z. A., & Ulusay, R. (2009). Water-induced variations in mechanical properties of clay-bearing rocks. International Journal of Rock Mechanics and Mining Sciences, 46(2), 355-370.

Erguvanlı, K., Yorulmaz, M., Çılı, F., Ahunbay, Z., Erdoğan M. (1989). Göreme yapısal koruma ve sağlamlaştırma projesi, E1 Nazar kilisesi, Istanbul Technical University (ITU), Faculty of Mining, Istanbul, 46 pp.

Evangelista, A. 1980. Influenza del contenuto d'acqua sul comportamento del tufo giallo napoletano. Atti del XIV Convegno Nazionale di Geotecnica, Firenze.

Evangelista, A., & Aversa, S. (1994). Experimental evidence of non-linear and creep behaviour of pyroclastic rocks. In Visco-Plastic Behaviour of Geomaterials (pp. 55-101). Springer, Vienna.

Evangelista, A., Aversa, S., Pescatore, T. S., & Pinto, F. (2000a). Soft rocks in southern Italy and role of volcanic tuffs in the urbanization of Naples. In Proceedings of the II International Symposium on 'The Geotechnics of Hard Soils and Soft Rocks', Napoli (Vol. 3, pp. 1243-1267).

Evangelista, A., Flora, A., Lirer, S., Feola, A., & Maiorano, R. M. S. (2000b). Numerical analysis of roof failure mechanisms of cavities in a soft rock. In ISRM International Symposium. International Society for Rock Mechanics.

Fedele, L., Scarpati, C., Sparice, D., Perrotta, A., & Laiena, F. (2016). A chemostratigraphic study of the Campanian Ignimbrite eruption (Campi Flegrei, Italy): insights on magma chamber withdrawal and deposit accumulation as revealed by compositionally zoned stratigraphic and facies framework. Journal of Volcanology and Geothermal Research, 324, 105-117.

Gatta, G. D., Cappelletti, P., & Langella, A. (2010). Crystal-chemistry of phillipsites from the Neapolitan Yellow Tuff. European Journal of Mineralogy, 22(6), 779-786.

Guarino, P. M., & Nisio, S. (2012). Anthropogenic sinkholes in the territory of the city of Naples (Southern Italy). Physics and Chemistry of the Earth, Parts A/B/C, 49, 92-102.

Guarino, P. M., Santo, A., Forte, G., De Falco, M., & Niceforo, D. M. A. (2018). Analysis of a database for anthropogenic sinkhole triggering and zonation in the Naples hinterland (Southern Italy). Natural Hazards, 91(1), 173-192.

Hall, S. A., De Sanctis, F., & Viggiani, G. (2006). Monitoring fracture propagation in a soft rock (Neapolitan Tuff) using acoustic emissions and digital images. Pure and Applied Geophysics, 163(10), 2171-2204.

Hawkes, I., & Mellor, M. (1970). Uniaxial testing in rock mechanics laboratories. Engineering Geology, 4(3), 179-285.

Heap, M. J., Lavallée, Y., Laumann, A., Hess, K. U., Meredith, P. G., & Dingwell, D. B. (2012). How tough is tuff in the event of fire? Geology, 40(4), 311-314.

Heap, M. J., Baud, P., Meredith, P. G., Vinciguerra, S., & Reuschlé, T. (2014). The permeability and elastic moduli of tuff from Campi Flegrei, Italy: implications for ground deformation modelling. Solid Earth, 5(1), 25.

Heidari, M., Khanlari, G. R., Torabi-Kaveh, M., Kargarian, S., & Saneie, S. (2014). Effect of porosity on rock brittleness. Rock mechanics and rock engineering, 47(2), 785-790.

Heiken, G. (Ed.). (2006). Tuffs: their properties, uses, hydrology, and resources (Vol. 408). Geological Society of America.

Hoek, E., & Brown, E. T. (1980). Underground excavations in rock, Institution of Mining and Metallurgy, London.

Jackson, M. D., Marra, F., Hay, R. L., Cawood, C., & Winkler, E. M. (2005). The judicious selection and preservation of tuff and travertine building stone in ancient Rome. Archaeometry, 47(3), 485-510.

Jackson, M. D., Kosso, C., Marra, F., & Hay, R. (2006). Geological basis of Vitruvius' empirical observations of material characteristics of rock utilized in Roman masonry.

In Proceedings of the Second International Congress of Construction History Queen's College, University of Cambridge (Vol. 2, 1685-1702).
Kleb, B., & Vásárhelyi, B. (2003). Test results and empirical formulas of rock mechanical parameters of rhyolitic tuff samples from Eger's cellars. Acta Geologica Hungarica, 46(3), 301-312.
Kilburn, C. R., De Natale, G., & Carlino, S. (2017). Progressive approach to eruption at Campi Flegrei caldera in southern Italy. Nature Communications, 8.
La Russa, M. F., Ruffolo, S. A., de Buergo, M. Á., Ricca, M., Belfiore, C. M., Pezzino, A., & Crisci, G. M. (2017). The behaviour of consolidated Neapolitan yellow Tuff against salt weathering. Bulletin of Engineering Geology and the Environment, 76(1), 115-124.
López-Doncel, R., Wedekind, W., Dohrmann, R., & Siegesmund, S. (2013). Moisture expansion associated to secondary porosity: an example of the Loseros Tuff of Guanajuato, Mexico. Environmental Earth Sciences, 69(4), 1189-1201.
Marmoni, G. M., Martino, S., Heap, M. J., & Reuschlé, T. (2017a). Gravitational slope-deformation of a resurgent caldera: New insights from the mechanical behaviour of Mt. Nuovo tuffs (Ischia Island, Italy). Journal of Volcanology and Geothermal Research. https://doi.org/10.1016/j.jvolgeores.2017.07.019.
Marmoni, G. M., Martino, S., Heap, M. J., & Reuschlé, T. (2017b). Multiphysics Laboratory Tests for Modelling Gravity-Driven Instabilities at Slope Scale. Procedia engineering, 191, 142-149.
Martin, R. J., Boyd, P. J., Noel, J. S., & Price, R. H. (1994). Bulk and mechanical properties of the Paintbrush Tuff recovered from Borehole USW NRG-6: data report (No. SAND—93-4020). Sandia National Labs., Albuquerque, NM (United States).
Mayer, K., Scheu, B., Montanaro, C., Yilmaz, T. I., Isaia, R., Aßbichler, D., & Dingwell, D. B. (2016). Hydrothermal alteration of surficial rocks at Solfatara (Campi Flegrei): petrophysical properties and implications for phreatic eruption processes. Journal of Volcanology and Geothermal Research, 320, 128-143.
Montanaro, C., Scheu, B., Mayer, K., Orsi, G., Moretti, R., Isaia, R., & Dingwell, D. B. (2016). Experimental investigations on the explosivity of steam-driven eruptions: A case study of Solfatara volcano (Campi Flegrei). Journal of Geophysical Research: Solid Earth, 121(11), 7996-8014.
Morra, V., Calcaterra, D., Cappelletti, P., Colella, A., Fedele, L., de' Gennaro, R., Langella, A., Mercurio, M., de' Gennaro, M. (2010). Urban geology: relationships between geological setting and architectural heritage of the Neapolitan area. In: (Eds.) Marco Beltrando, Angelo Peccerillo, Massimo Mattei, Sandro Conticelli, and Carlo Doglioni, Journal of the Virtual Explorer, volume 36, paper 26, doi: 10.3809/jvirtex.2010.00261.
Nijland, T. G., Van Hees, R. P., & Bolondi, L. (2010). Evaluation of three Italian tuffs (Neapolitan Yellow Tuff, Tufo Romano and Tufo Etrusco) as compatible replacement stone for Römer tuff in Dutch built cultural heritage. Geological Society, London, Special Publications, 333(1), 119-127.
Nocilla, N., Evangelista, A., & Di Santolo, A. S. (2009). Fragmentation during rock falls: two Italian case studies of hard and soft rocks. Rock mechanics and rock engineering, 42(5), 815.
Okubo, S. & Chu S. Y. (1994). Uniaxial compression creep of Tage and Oya tuff in air-dried and water-saturated conditions. J. Soc. Mat. Sci., Japan, 43(490), 819-825.
Orsi, G., D'Antonio, M., de Vita, S., & Gallo, G. (1992). The Neapolitan Yellow Tuff, a large-magnitude trachytic phreatoplinian eruption: eruptive dynamics, magma withdrawal and caldera collapse. Journal of Volcanology and Geothermal Research, 53(1), 275-287.
Orsi, G., De Vita, S., & Di Vito, M. (1996). The restless, resurgent Campi Flegrei nested caldera (Italy): constraints on its evolution and configuration. Journal of Volcanology and Geothermal Research, 74(3-4), 179-214.
Peluso, F., & Arienzo, I. (2007). Experimental determination of permeability of Neapolitan Yellow Tuff. Journal of volcanology and geothermal research, 160(1), 125-136.

583 Price, R. H. (1983). Analysis of the rock mechanics properties of volcanic tuff units from
584 Yucca Mountain, Nevada Test Site. Sandia National Laboratories.
585 Price, R. H., & Jones, A. K. (1982). Uniaxial and triaxial compression test series on Calico
586 Hills tuff (No. SAND—82-1314). Sandia National Labs., Albuquerque, NM (United
587 States).
588 Rosi, M., Vezzoli, L., Aleotti, P., & De Censi, M. (1996). Interaction between caldera
589 collapse and eruptive dynamics during the Campanian Ignimbrite eruption, Phlegraean
590 Fields, Italy. Bulletin of Volcanology, 57(7), 541-554.
591 Scarpati, C., Cole, P., & Perrotta, A. (1993). The Neapolitan Yellow Tuff—a large volume
592 multiphase eruption from Campi Flegrei, southern Italy. Bulletin of Volcanology,
593 55(5), 343-356.
594 Schmitt, L., Forsans, T., & Santarelli, F. J. (1994). Shale testing and capillary phenomena.
595 In International Journal of Rock Mechanics and Mining Sciences & Geomechanics
596 Abstracts (Vol. 31, No. 5, pp. 411-427). Pergamon.
597 Schultz, R. A., & Li, Q. (1995). Uniaxial strength testing of non-welded Calico Hills tuff,
598 Yucca Mountain, Nevada. Engineering geology, 40(3-4), 287-299.
599 Shakoor, A., & Barefield, E. H. (2009). Relationship between unconfined compressive
600 strength and degree of saturation for selected sandstones. Environmental &
601 Engineering Geoscience, 15(1), 29-40.
602 Stück, H., Forgó, L. Z., Rüdrich, J., Siegesmund, S., & Török, A. (2008). The behaviour of
603 consolidated volcanic tuffs: weathering mechanisms under simulated laboratory
604 conditions. Environmental geology, 56(3-4), 699-713.
605 Topal, T., & Doyuran, V. (1997). Engineering geological properties and durability assessment
606 of the Cappadocian tuff. Engineering Geology, 47(1-2), 175-187.
607 Topal, T., & Sözmen, B. (2003). Deterioration mechanisms of tuffs in Midas
608 monument. Engineering Geology, 68(3), 201-223.
609 Török, A., Gálos, M., & Kocsanyi-Kopecsko, K. (2004). Experimental weathering of rhyolite
610 tuff building stones and the effect of an organic polymer conserving agent. Stone
611 Decay: Its Causes and Controls, 109-127.
612 Tuncay, E. (2009). Rock rupture phenomenon and pillar failure in tuffs in the Cappadocia
613 region (Turkey). International Journal of Rock Mechanics and Mining Sciences, 46(8),
614 1253-1266.
615 Vásárhelyi, B. (2002). Influence of the water saturation on the strength of volcanic tuffs.
616 In ISRM International Symposium-EUROCK 2002. International Society for Rock
617 Mechanics.
618 Wedekind, W., López-Doncel, R., Dohrmann, R., Kocher, M., & Siegesmund, S. (2013).
619 Weathering of volcanic tuff rocks caused by moisture expansion. Environmental earth
620 sciences, 69(4), 1203-1224.
621 Wohletz, K., Orsi, G., & De Vita, S. (1995). Eruptive mechanisms of the Neapolitan Yellow
622 Tuff interpreted from stratigraphie, chemical, and granulometric data. Journal of
623 Volcanology and Geothermal Research, 67(4), 263-290.
624 Yassaghi, A., Salari-Rad, H., & Kanani-Moghadam, H. (2005). Geomechanical evaluations of
625 Karaj tuffs for rock tunnelling in Tehran–Shomal Freeway, Iran. Engineering
626 Geology, 77(1), 83-98.
627 Yavuz, A. B. (2012). Durability assessment of the Alaçatı tuff (Izmir) in western
628 Turkey. Environmental Earth Sciences, 67(7), 1909-1925.
629 Zhu, W., Baud, P., Vinciguerra, S., & Wong, T.-f. (2011). Micromechanics of brittle faulting
630 and cataclastic flow in Alban Hills tuff. Journal of Geophysical Research: Solid
631 Earth, 116(B6).
632

Mineral	Mineral content [wt.%]
Amorphous phase	36 ± 5
K-feldspar	10 ± 1
Biotite	2 ± 1
Clinopyroxene	3 ± 1
Chabazite	30 ± 2
Phillipsite	16 ± 2
Smectite	3 ± 1

633

634 **Table 1.** Quantitative bulk mineralogical composition, determined using X-ray

635 powder diffraction (XRPD), for the Neapolitan Yellow Tuff used in this study.

Sample	Sample diameter [mm]	Connected porosity	Uniaxial compressive strength [MPa]	Experimental condition	Uniaxial compressive strength (diameter = 50 mm) (Equation 1) [MPa]
NYT-1	19.83	0.46	3.71	Wet	3.14
NYT-2	19.82	0.46	5.76	Dry	4.88
NYT-3	19.87	0.44	4.60	Wet	3.90
NYT-4	19.77	0.47	4.87	Dry	4.12
NYT-5	19.83	0.47	3.28	Wet	2.78
NYT-6	19.86	0.45	4.96	Dry	4.20
NYT-8	19.84	0.46	5.32	Dry	4.51
NYT-9	19.84	0.45	3.64	Wet	3.08
NYT-10	19.86	0.45	6.26	Dry	5.30
NYT*-1	19.86	0.46	4.29	Wet	3.63
NYT25-1	24.97	0.47	2.87	Wet	2.53
NYT25-2	24.93	0.47	2.59	Wet	2.29
NYT25-3	25.58	0.46	3.73	Wet	3.31
NYT25-4	24.97	0.47	4.16	Wet	3.67
NYT25-5	24.98	0.46	3.40	Wet	3.00
NYT25-6	25.58	0.46	3.81	Wet	3.38
NYT25-7	24.95	0.45	3.07	Wet	2.71
NYT25-8	24.92	0.45	3.65	Wet	3.22
NYT25-9	25.42	0.46	3.06	Wet	2.71
NYT25-10	25.00	0.47	2.58	Wet	2.28
NYT25-11	24.93	0.45	6.23	Dry	5.50
NYT25-12	25.48	0.46	5.22	Dry	4.62
NYT25-13	25.58	0.46	5.26	Dry	4.66
NYT25-14	24.79	0.45	5.59	Dry	4.93
NYT25-15	24.89	0.45	5.48	Dry	4.83
NYT25-16	24.90	0.45	6.78	Dry	5.98
NYT25-17	24.98	0.46	6.00	Dry	5.30
NYT25-19	25.56	0.46	4.77	Dry	4.23

Table 2. Summary of the 28 experiments performed on Neapolitan Yellow Tuff (NYT) for this study. Wet – vacuum-saturated in deionised water (see text for details). Dry – dried in a vacuum oven at 40 °C for at least 48 h. The uniaxial compressive strength for a sample of 50 mm diameter was calculated using the empirical relation given as Equation (1) (see text for details). The average connected porosities for the samples deformed in the dry and wet condition are 0.456 and 0.459, respectively.

Tuff	Outcrop	Connected porosity	±	UCS_{dry} [MPa]	±	UCS_{wet} [MPa]	±	$\frac{UCS_{wet}}{UCS_{dry}}$	Source	Notes
Anatolian tuff	White	0.39	0.008	10.00	0.88	3.76	0.53	0.376	Topal and Sözmen (2003)	No zeolites. Smectite and Illite present
	Pink	0.33	0.021	16.95	0.54	10.89	1.82	0.642		No zeolites. Smectite, Illite, and Kaolinite present
	White	0.28		8.15		3.55		0.436	Ayday and Göktan (1990)	No zeolites. Smectite and Illite present
	Pink	0.24		18.23		10.46		0.574		No zeolites. Smectite, Illite, and Kaolinite present
Cappadoccian tuff	Vertical	0.38	0.005	6.53	0.67	2.16	0.34	0.331	Topal and Doyuran (1997)	Volcanic glass shards are partly altered to smectite
	Horizontal	0.38	0.005	4.87	0.43	0.93	0.29	0.191		
	Vertical	0.29		6.50		3.00		0.462	Erdoğan (1986)	
	Vertical	0.29		6.50		3.00		0.462	Erguvanlı et al. (1989)	
	Kavak	0.27		3.60		1.10		0.306	Tuncay (2009)	Clinoptilolite
		0.21		5.00		1.56		0.312		
		0.24		5.00		1.33		0.266		
	Zelve	0.26		4.20		0.83		0.198		Substantially clinptilolite-rich, but also containing minor erionite, chabazite and phillipsite[1]
	Cemilköy	0.35		1.20		0.44		0.367		
		0.28		2.20		0.52		0.236		
	Kızılkaya	0.27		6.30		3.88		0.616		No zeolites
		0.37		3.40		3.27		0.962		
	Ortahisar	0.34		6.60		1.30		0.197	Erguler and Ulusay (2009)	81 % clay (montmorillonite)
	Ürgüp	0.26		12.90		1.60		0.124		27% clay minerals
		0.26		9.70		1.30		0.134		40% clay minerals
Yucca Mountain tuff	Calico Hills	0.30	0.015	29.09	3.19	5.34	0.77	0.184	Schultz and Li (1995)	Low temperature zeolitic alteration products in Calico Hills rocks include clinoptilolite zeolite, mordenite and smectite[2]

[1] Cejka et al. (2007); Temel and Gündoğdu (1994)
[2] Broxton et al. (1993)

		0.38		36.85	4.15	30.40	7.45	0.825	Price (1982); Price and Jones (1982)	
	Paintbrush tuff	0.40	0.011	4.70	1.20	11.30		2.404	Martin et al. (1994)	Heulandite-clinoptilolite and smectite[3]
Karaj tuff	Crystalline	0.10	0.005	121.00	21.00	92.00	14.00	0.760	Yassaghi et al. (2005)	No zeolites
	Vitric	0.13	0.022	92.50	12.50	52.00	3.00	0.562		20% clay minerals
	Lithic	0.09	0.023	98.50	11.50	64.50	6.50	0.655		45% clay minerals
Mt. Nuovo	Upper unit	0.46	0.021	4.85	0.45	2.68	0.88	0.552	Marmoni et al. (2017a)	Glass partially replaced by zeolites (incl. analcime and phillipsite)
	Lower unit	0.21	0.005	33.77	4.03	26.00		0.770		
Urumieh-Dokhtar tuff		0.03		124.30		78.20		0.629	Heidari et al. (2014)	Data not available
Challis tuff	Perpendicular to bedding	0.24		75.01		29.27		0.390	Behre Jr. (1929)	Contains montmorillonite clay andmordenite (zeolite)[4]
	Parallel to bedding	0.24		78.92		28.52		0.361		
Alaçatı tuff		0.26	0.009	14.90	1.95	6.90	1.03	0.463	Yavuz (2012)	Contains smectite and mordenite
Ayazini tuff		0.37	0.022	22.21	1.47	12.44	0.49	0.560	Çelik et al. (2014)	Illite and smectite present
Seydiler tuff		0.36	0.027	19.07	1.69	9.07	0.25	0.476	Çelik and Ergul (2015)	
Sárospatak rhyolite tuff		0.20		19.47		8.95		0.460	Török et al. (2004)	Montmorillonite and other clay minerals
Oya tuff		0.34		11.20	0.92	5.00	0.51	0.446	Okubo and Chu	Contains clinoptilolite and mordenite

[3] Levy and O'Neil (1989)
[4] Ross and Shannon (1924)

Tage tuff		0.25		16.10	0.92	9.10	0.59	0.565	(1994)	
Monti Sabatini tuff	Tufo Giallo della Prima Porta	0.23		20.40	0.35	9.80	0.11	0.480	Jackson et al. (2005)	Analcime, phillipsite, and chabazite
	Tufo Giallo della Via Tibernia	0.20		22.90	0.94	7.60	0.05	0.332		
Monti Albani tuff	Tufo Lionato	0.15		28.50	0.68	15.90	0.40	0.558		
	Lapis Albanus	0.11		31.30	0.25	16.30	0.39	0.521		
	Tufo di Tusculo	0.15		36.70	1.80	17.30	0.48	0.471		
	Lapis Gabinus	0.14		39.50	4.15	15.50	0.53	0.392		
	Peperino della Via Flaminia	0.13		43.40	6.21	28.80	3.48	0.664		
	Pisolitico di Trigoria	0.35	0.002					0.500[5]	Zhu et al. (2011)	Phillipsite and chabazite
	Palatino	0.32	0.004					0.683[6]		
Eger-Demjén tuff		0.19		39.75		25.96		0.653	Vásárhelyi, (pers. Comm.)	Contains 10-20% smectite[7]
		0.40		8.49		3.35		0.395		
		0.39		4.95		1.59		0.321		
		0.51		3.03		0.74		0.244		
		0.37		7.61		2.60		0.342		
		0.36		6.11		1.37		0.224		
		0.36		5.60		1.91		0.341		
		0.38		7.66		2.24		0.292		
		0.40		4.67		1.74		0.373		
		0.58		2.59		1.15		0.444		
		0.34		8.40		2.76		0.329		
		0.38		4.40		0.87		0.198		
		0.39		5.54		2.02		0.365		
		0.41		3.53		0.55		0.156		
		0.34		5.32		2.21		0.415		
		0.35		7.81		2.94		0.376		

[5] Estimated from P* wet/dry ratio
[6] Estimated from P* wet/dry ratio
[7] Wedekind et al. (2013)

		0.37		3.13		0.63		0.201		
		0.38		5.36		1.20		0.224		
Tuff from Hungary	Rhyolite tuff	0.45		2.59		1.18		0.444	Vásárhelyi (2002)	Data not available
		0.30		4.95		1.59		0.321		
		0.32		4.69		1.74		0.371		
		0.29		5.54		2.02		0.365		
		0.27		5.60		1.91		0.341		
		0.30		8.49		3.35		0.395		
		0.30		7.66		2.24		0.292		
		0.30		10.03		7.83		0.781		
		0.28		7.81		2.94		0.376		
		0.29		5.36		1.20		0.224		
		0.29		21.81		21.27		0.975		
		0.15		39.75		26.90		0.677		
	Andesite tuff	0.20		26.00		20.20		0.78		
		0.15		33.50		27.74		0.83		
		0.17		30.33		22.32		0.74		
		0.16		16.30		8.62		0.53		
		0.07		32.60		21.50		0.66		
		0.11		19.80		10.10		0.51		
		0.08		15.60		11.30		0.72		
		0.14		28.60		19.80		0.69		
	Basalt tuff	0.27		8.50		8.30		0.98		
		0.20		3.34		2.48		0.74		
		0.30		3.05		1.76		0.58		
		0.22		4.36		3.40		0.78		
		0.31		8.30		14.04		1.69		
		0.24		8.34		12.88		1.54		
		0.00		3.83		3.10		0.81		
		0.09		14.12		13.07		0.93		
		0.09		40.29		18.43		0.46		
		0.03		63.36		53.2		0.84		
Neapolitan Yellow Tuff		0.49	0.011	6.65	0.65	1.88	0.68	0.28	Montanaro et al. (2016)	Zeolites

La Pietra Tuff 1		0.49	0.004	4.56	0.94	2.27	0.97	0.50		
La Pietra Tuff 2		0.47	0.013	9.74	0.84	3.68	1.32	0.38		
Gauro Tuff		0.46	0.009	11.78	1.17	4.82	0.49	0.41		
Neapolitan Yellow Tuff (this study)	Monte San Severino	0.46	0.017	5.44	0.83	3.81	0.79	0.701	This study	Phillipsite, chabazite, and smectite
Grey Campanian Ignimbrite (WGI; this study)	open quarry to the north-west of the town of Caserta (Italy)	0.50	0.005	10.59	1.31	9.94	1.04	0.939		No zeolites or clays present
Piperno tuff (PT; this study)	open quarry in the Neapolitan area (Italy)	0.51	0.004	3.17		3.29		1.038	This study	No zeolites or clays present

644

645 **Table 3**. Summary of the published (including data from this study) wet and dry uniaxial compressive strength of tuffs from around the globe.

646 UCS_{dry} – dry uniaxial compressive strength; UCS_{wet} – wet uniaxial compressive strength.

647

Tuff	Outcrop	Connected porosity	±	τ_{dry} [MPa]	±	τ_{wet} [MPa]	±	$\frac{\tau_{wet}}{\tau_{dry}}$	Source	Notes
Eger-Demjén		0.35	0.010	3.30	0.57	2.78	0.36	0.844	Stück et al. (2008)	Data not available
Eger-Tihamér		0.36	0.002	0.81	0.14	0.31	0.08	0.386		
Weibern tuff		0.43	0.004	1.64	0.22	1.23	0.14	0.754		Fine grained matrix of zeolite minerals
Rochlitz tuff		0.28	0.005	2.42	0.28	1.47	0.26	0.608		Presence of kaolinite
Habichtswald tuff		0.22	0.013	2.68	0.91	2.37	0.6	0.887		Smectite-zeolite matrix
Loseros tuff	X	0.07		6.29		5.82		0.925	Wedekind et al. (2013)	Kaolinite, illite, and smectite
	Z	0.07		8.25		6.69		0.811		
Cantera Rosa tuff	X	0.41		3.94		2.61		0.662		Smectite and kaolinite
	Z	0.41		4.02		3.00		0.746		
Chiluca tuff	X	0.08		5.13		4.56		0.889		Small amounts of illite and smectite
	Z	0.08		5.61		4.79		0.854		
Gris de los Remedios tuff	X	0.31		2.27		1.39		0.612		Smectites and traces of muscovite/illite
	Z	0.31		2.24		1.58		0.773		
Cantera Formación tuff	X	0.13		10.65		8.23		0.773		Kaolinite and halloysite

	Z	0.13		9.89		8.71		0.881		
Cantera Blanca tuff	X	0.15		6.90		3.99		0.578		Mordenite, clinoptilolite, and montmorillonite
	Z	0.15		5.89		3.11		0.528		
Bufa tuff	X	0.18		6.04		3.65		0.604		Illite and smectite
	Z	0.18		6.95		4.57		0.658		
Tenayocátetl tuff	X	0.05		5.43		3.94		0.726		Smectite
	Z	0.05		5.71		4.12		0.722		
Cantera Amarilla tuff	X	0.42		0.99		0.49		0.495		Smectite, kaolinite, and halloysite
	Z	0.42		1.05		0.56		0.533		
Hilbersdorf tuff	X	0.30		3.70		1.14		0.308		Illite
	Z	0.30		4.62		3.10		0.671		

Table 4. Summary of the published wet and dry tensile strengths of tuffs from around the globe. τ_{dry} – dry tensile strength; τ_{wet} – wet tensile strength.

Sample	Sample diameter [mm]	Connected porosity	Uniaxial compressive strength [MPa]	Experimental condition	Uniaxial compressive strength (diameter = 50 mm) (Equation 1) [MPa]
PIP-1	20.26	0.51	3.17	Dry	2.69
PIP-2	20.29	0.50	3.29	Wet	2.80
CI-4	19.85	0.50	10.97	Wet	9.29
CI-9	19.79	0.50	9.54	Wet	8.07
CI-10	19.82	0.50	9.59	Wet	8.12
CI-11	19.83	0.50	9.65	Wet	8.17
CI-13	19.81	0.50	10.88	Dry	9.21
CI-19	19.81	0.50	10.17	Dry	8.61
CI-20	19.83	0.50	11.05	Dry	9.36
CI-21	19.83	0.50	8.95	Dry	7.58
CI-22	19.84	0.50	11.90	Dry	10.08
CI*-2	19.83	0.50	10.94	Wet	9.26

Table 5. Summary of the experiments performed on Piperno Tuff (labelled "PIP") and the grey Campanian Ignimbrite (labelled "CI") for this study. Wet – vacuum-saturated in deionised water (see text for details). Dry – dried in a vacuum oven at 40 °C for at least 48 h. The uniaxial compressive strength for a sample of 50 mm diameter was calculated using the empirical relation given as Equation (1) (see text for details).

660 **Figure captions**

661

662 **Figure 1**. Maps showing the location of Naples (inset is a map of Italy). The inferred
663 Campi Flegrei caldera is indicated by the dashed circle, and the main towns with blue
664 dots. The Neapolitan Yellow Tuff (NYT) used in this study was collected from an
665 open quarry at Monte San Severino, on the border of the inferred Campi Flegrei
666 caldera.

667

668 **Figure 2.** Photographs of buildings constructed using Neapolitan Yellow Tuff (NYT)
669 in Naples. (a) Castel dell'Ovo, (b) Castel Nuovo, (c) the church of Santa Chiara, (d)
670 the church of San Domenico Maggiore, (e) the Academy of Fine Arts, and (f) a
671 plastered wall constructed using NYT within the ancient city centre of Naples.

672

673 **Figure 3**. (a) Weathering on a wall constructed using Neapolitan Yellow Tuff (NYT)
674 within the ancient city centre of Naples. (b) and (c) Weathering on NYT walls within
675 the Castel dell'Ovo.

676

677 **Figure 4**. A photograph (a) and an optical photomicrograph (b) of the Neapolitan
678 Yellow Tuff (NYT) used in this study (modified from Heap et al., 2012). A K-
679 feldspar and clinopyroxene phenocryst and a porous juvenile lapilli fragment are
680 labelled on the photomicrograph.

681

682 **Figure 5**. (a) Pore throat diameter distribution for the Neapolitan Yellow Tuff (NYT)
683 determined using mercury porosimetry. (b) Representative uniaxial stress-strain
684 curves for a sample of wet (blue curve) and dry (black curve) NYT. (c) Uniaxial

685 compressive strength (UCS) as a function of connected porosity for the NYT. Error
686 associated with transducer precision is within the size of the symbols.
687
688 **Figure 6**. (a) Water-weakening (ratio of wet to dry strength) as a function of porosity
689 for tuffs all over the world. (b) Ratio of wet to dry uniaxial compressive strength as a
690 function of porosity (data for which the composition is known). Data are in three
691 groups (1) tuffs that contain zeolites (white circles), (2) tuffs that contain clays but no
692 zeolites (grey circles), and (3) tuffs that contain neither zeolites nor clays (black
693 circles). Data from: this study, Behre Jr. (1929), Price (1982), Price and Jones (1982),
694 Erdoğan (1986), Erguvanlı et al. (1989), Ayday and Göktan (1990), Martin et al.
695 (1994), Okubo and Chu (1994), Schultz and Li (1995), Topal and Doyuran (1997),
696 Vásárhelyi (2002), Topal and Sözman (2003), Török et al. (2004), Yassaghi et al.
697 (2005), Jackson et al. (2005), Tuncay (2009), Stück et al. (2008), Erguler and Ulusay
698 (2009), Zhu et al. (2011), Heidari et al. (2013), Wedekind et al. (2013), Çelik et al.
699 (2014), Çelik and Ergul (2015), Montanaro et al. (2016), Marmoni et al. (2017a), and
700 Vásárhelyi (pers. comm.).
701
702 **Figure 7**. (a) Photograph of the church of Gesù Nuovo in Naples. (b) Photograph of
703 front of the church of Gesù Nuovo showing the pyramid-shaped bossage constructed
704 using Piperno Tuff.

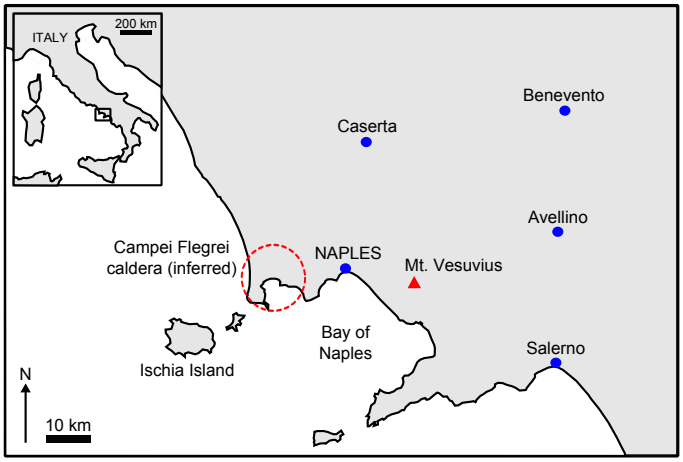

Figure 1; Heap et al.


a)


b)


c)


d)


e)


f)


a)


b)


c)

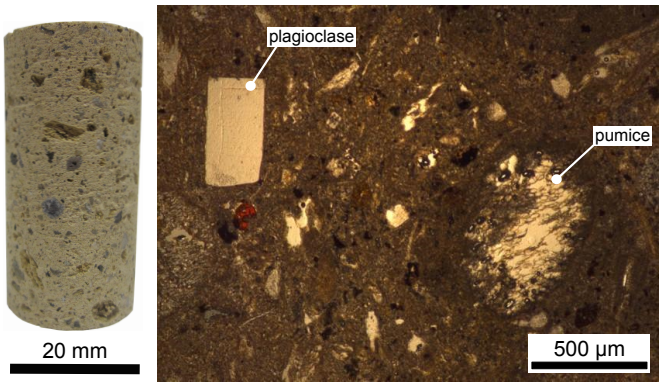

Figure 4; Heap et al.

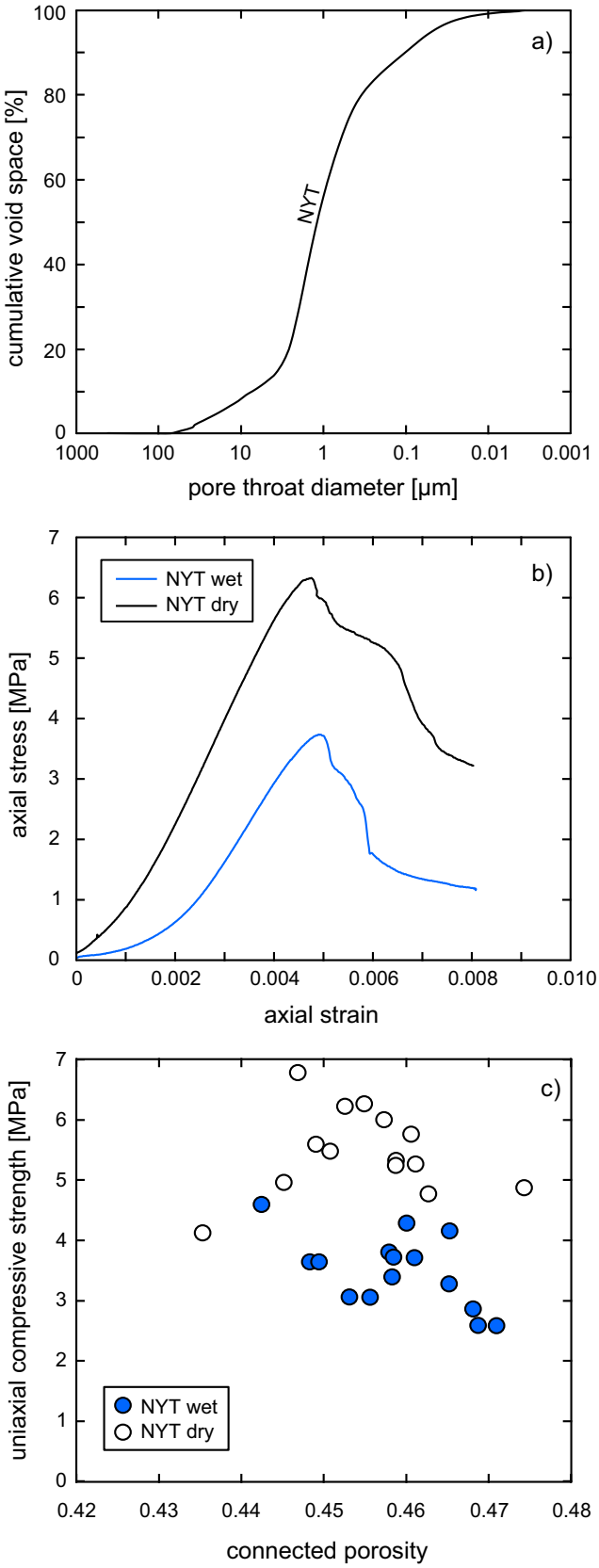
a)
cumulative void space [%]
pore throat diameter [µm]
NYT
b)
NYT wet
NYT dry
axial stress [MPa]
axial strain
c)
uniaxial compressive strength [MPa]
connected porosity
NYT wet
NYT dry

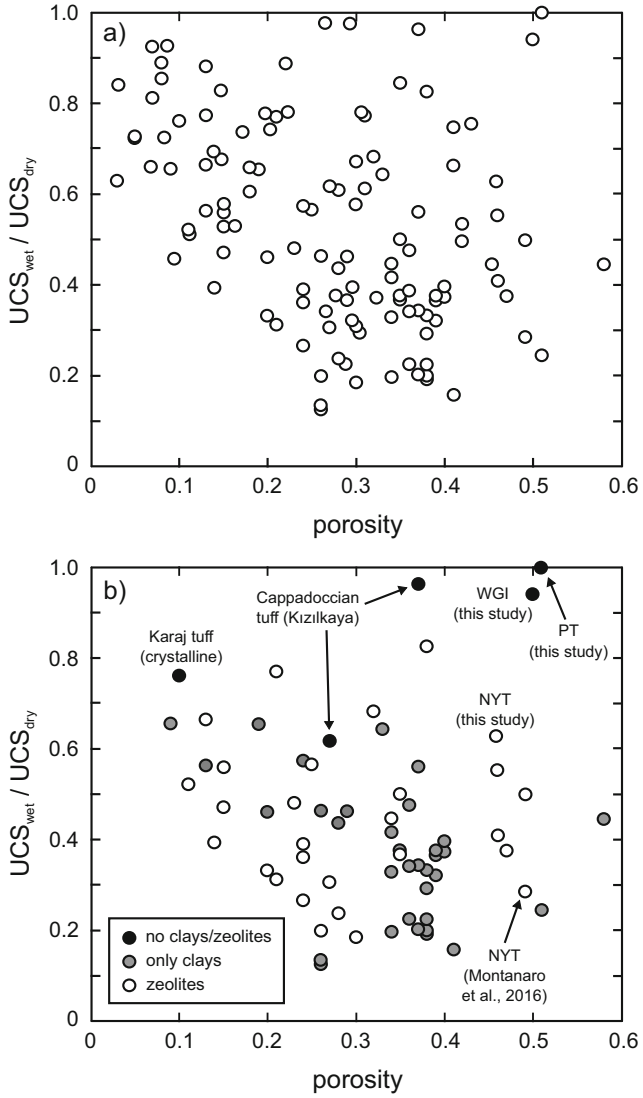
a)
1.0
0.8
0.6
0.4
0.2
0
0
0.1
0.2
0.3
0.4
0.5
0.6
porosity
UCS$_{wet}$ / UCS$_{dry}$
b)
Cappadoccian
tuff (Kızılkaya)
WGI
(this study)
PT
(this study)
Karaj tuff
(crystalline)
NYT
(this study)
NYT
(Montanaro
et al., 2016)
no clays/zeolites
only clays
zeolites
1.0
0.8
0.6
0.4
0.2
0
0
0.1
0.2
0.3
0.4
0.5
0.6
porosity
UCS$_{wet}$ / UCS$_{dry}$